

Porous Organic Cage as an Efficient Platform for Industrial Radioactive Iodine Capture

Xiongli Liu, Zhiyuan Zhang, Feng Shui, Shuo Zhang, Lin Li, Junhua Wang, Mao Yi, Zifeng You, Shiqi Yang, Rufeng Yang, Shan Wang, Yilian Liu, Qiao Zhao, Baiyan Li,* Xian-He Bu,* and Shengqian Ma*

Abstract: Herein, we firstly develop porous organic cage (POC) as an efficient platform for highly effective radioactive iodine capture under industrial operating conditions (typically $\geq 150^\circ\text{C}$), ≤ 150 ppmv of I_2). Due to the highly dispersed and readily accessible binding sites as well as sufficient accommodating space, the constructed NKPOC-DT-(I^-) (NKPOC=Nankai porous organic cage) demonstrates a record-high I_2 uptake capacity of 48.35 wt % and extraordinary adsorption capacity of unit ionic site (~ 1.62) at 150°C and 150 ppmv of I_2 . The I_2 capacity is 3.5, 1.6, and 1.3 times higher than industrial silver-based adsorbents Ag@MOR and benchmark materials of TGDM and 4F-iCOF-TpBpy- I^- under the same conditions. Furthermore, NKPOC-DT-(I^-)Me exhibits remarkable adsorption kinetics ($k_1 = 0.013 \text{ min}^{-1}$), which is 1.2 and 1.6 times higher than TGDM and 4F-iCOF-TpBpy- I^- under the identical conditions. NKPOC-DT-(I^-)Me thus sets a new benchmark for industrial radioactive I_2 adsorbents. This work not only provides a new insight for effectively enhancing the adsorption capacity of unit functional sites, but also advances POC as an efficient platform for radioiodine capture in industry.

Introduction

Radioactive species including ^{99}Tc , ^3H , ^{85}Kr , ^{137}Cs , ^{133}Xe , $^{129}\text{I}_2$, ^{238}U , ^{237}Np , ^{242}Pu , ^{243}Am , etc., in nuclear waste, often show negative impacts on the environment and living organisms due to their radioactivity, teratogenicity, and carcinogenicity.^[1] Especially, radioactive molecular iodine ($^{129}\text{I}_2$) as one of the main volatile wastes, can produce detrimental effects on environmental safety and human health due to their intrinsic high toxicity, long half-decay cycle ($\sim 1.57 \times 10^7$ years), high mobility, and high biological activity, which must be captured and sequestered immediately.^[2] The reprocessing of nuclear fuel rods would produce a low concentration of $^{129}\text{I}_2$ (often ≤ 150 ppmv) and require a high-temperature environment (typically $\geq 150^\circ\text{C}$) for accelerating the dissolution of fuel rods and decreasing the competitive adsorption of water molecules.^[3] Therefore, it is an urgent task to develop advanced materials for I_2 capture at high temperature and low I_2 concentration.

The ideal industrial iodine adsorbent should possess the following features: (i) high chemical and thermal stability to satisfy the requirements of acidity and high temperature environments of industrial operating conditions;^[4] (ii) highly dispersed and readily accessible strong functional sites to guarantee a high adsorption capacity and outstanding decontamination factor without I_2 leakage under high temperature; (iii) large and easily accessible pore window for improving adsorption kinetics; (iv) excellent recyclability to reduce the operating cost; (v) simple synthesis method to meet the practical requirement of industrial applications.

The current industrial technology for $^{129}\text{I}_2$ capture relies on silver-based adsorbents,^[5] whose key lies in their ability to effectively bind I_2 with high decontamination performance under high temperature (eg. $\geq 150^\circ\text{C}$) and low I_2 concentration (eg. ≤ 150 ppmv of I_2), a practical conditions for industrial radioactive iodine capture.^[6] However, current silver based adsorbents suffer from low uptake capacity (eg. Ag@MOR) and poor recyclability due to their low surface area and irreversible chemical reaction between silver and iodine to form AgI.^[7] This would result in the potential inefficiency and high operating cost under long-term operation, especially when operated in nuclear energy facilities with limited space.^[8] Even if a large number of efforts have been devoted to realize industrial substitution of silver-based adsorbents, the developed porous adsorbents including activated carbon,^[9] metal-organic frameworks

[*] Dr. X. Liu, Z. Zhang, F. Shui, Dr. L. Li, Dr. J. Wang, M. Yi, Z. You, S. Yang, R. Yang, S. Wang, Y. Liu, Dr. Q. Zhao, Prof. Dr. B. Li, Prof. Dr. X.-H. Bu
School of Materials Science and Engineering, National Institute for Advanced Materials, TKL of Metal and Molecule-Based Material Chemistry
Nankai University
Tianjin 300350, P. R. China
E-mail: libaiyan@nankai.edu.cn
buxh@nankai.edu.cn

Prof. Dr. S. Ma
Department of Chemistry
University of North Texas
1508 W Mulberry St, Denton, TX 76201, USA
E-mail: Shengqian.Ma@unt.edu

Dr. S. Zhang
College of Materials Science and Engineering
Qingdao University of Science and Technology
Qingdao 266042, P. R. China

(MOFs),^[2b,10] porous organic polymers (POPs),^[11] covalent organic frameworks (COFs),^[12] and hydrogen-bonded cross-linked organic frameworks (HCOFs),^[13] only exhibit high I_2 uptake capacities at moderate temperatures ($\leq 90^\circ\text{C}$) and high I_2 concentrations (> 10000 ppmv), which is far from the practical industrial requirements. To the best of our knowledge, only four limited cases including TGDM (a 2D guanidinium COF),^[14] 4F-iCOF-TpBpy-I⁻ and 4CH₃-iCOF-TpBpy-I⁻ (a 2D COF with both ionic sites and Lewis base sites),^[15] and JUC-561 (a sulfur functionalized COF with redox sites^[12c]) exhibit the exceeding I_2 uptake over traditional silver-based adsorbents under industrial operating conditions.^[3,12c, 16]

Compared to reported redox sulfur sites in porous adsorbents, ionic sites are considered to have stronger binding interactions towards iodine due to strong Coulombic force.^[14–15] However, the reported ionic adsorbents have always been limited to the ability that each ionic site can only bind less than one iodine molecule under high temperature, which may attribute to the existence of underutilized ionic binding sites including “co-occupied binding sites” and/or “invalid binding sites” in reported 2D COFs caused by their congested ionic sites between layers (Figure 1a). Even if the utilization of 3D COFs seems a probable choice to reduce the crowded arrangement of ionic sites, the uncontrollable interpenetrating remains a significant obstacle to obtaining highly dispersed ion functional sites in 3D COFs.^[17] Thus, it is necessary to develop new types of porous adsorbents with highly dispersed and sufficiently

utilized ionic sites for capturing radioactive iodine under industrial operating conditions.

Porous organic cages (POCs), an emerging class of crystalline porous materials, have been previously applied in the fields of gas storage and separation,^[18] catalysis,^[19] and pollutant treatment.^[20] Similar to MOFs and COFs, POCs not only contain the advantageous features for guest capture including high surface areas, adjustable porosities, and easily functional modification, but also possess the unique advantages of highly dispersed and readily accessible sites (Figure 1b) due to their intrinsically cave-like discrete structures that are not easily interpenetrating.^[21] However, although POCs have been developed for over a decade, their application for radioactive I_2 capture under industrial conditions has been unexplored. Herein, we showcase for the first time the development of POCs as a new industrial radioactive I_2 capture platform outperforming some benchmark materials.

To effectively enhance the I_2 adsorption performance, a nitrogen-rich POC (NKPOC-DT, NKPOC = Nankai porous organic cage) was quaternized to form ionic POC, namely NKPOC-DT-(I⁻)Me (Figure 2). Due to highly dispersed functional sites in POC, NKPOC-DT-(I⁻)Me exhibits a record-high I_2 uptake capacity of 48.35 wt% among all reported porous materials under industrial operating conditions, which is 3.2 times higher than its parent material of NKPOC-DT (15.12 wt%). It is 3.5, 1.6, and 1.3 times higher than that of industrial silver-based adsorbents Ag@MOR and benchmark materials of TGDM and 4F-iCOF-TpBpy-I⁻ under the same conditions. Each ionic sites in NKPOC-DT-(I⁻)Me can capture over 1.62 equivalent of iodine molecules, far exceeding the reported COFs adsorbents (~ 0.44 I_2 /ionic site for TGDM and 0.76 I_2 /ionic site for 4F-iCOF-TpBpy-I⁻).^[14–15] Furthermore, NKPOC-DT-(I⁻)Me exhibits a remarkably high adsorption kinetics with adsorption rate of 0.013 min^{-1} , and outperforms the benchmarked materials of TGDM and 4F-iCOF-TpBpy-I⁻. NKPOC-DT-(I⁻)Me, thus setting a new benchmark for radioactive I_2 adsorbents under industrial conditions.

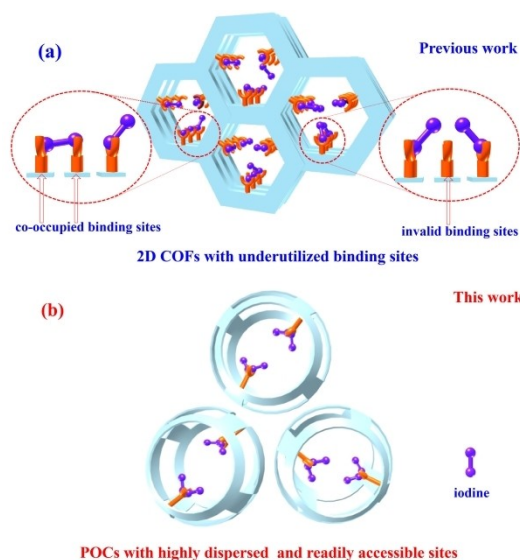


Figure 1. The comparison of benchmark 2D COF model and the designed POC for capturing radioactive iodine under industrial operating conditions. (a) The underutilized binding sites in 2D COFs including “co-occupied binding sites” and “invalid binding sites” due to the crowded arrangements of binding sites between layers; (b) the “highly dispersed” and “readily accessible sites” in POC can provide the sufficient accommodation space for adsorbed more I_2 molecules, thus effectively improving the adsorption ability of unit ionic sites.

Results and Discussion

Synthesis and Characterization

The triazole-connected POC (NKPOC-DT) was synthesized by reacting tetraformylresorcin-[4]arene (C4RACHO) with 3,5-diamino-1,2,4-triazole (DT) in pressure flask at 100°C for 24 h using *N,N*-dimethylformamide (DMF) as solvent. The powder X-ray diffraction (PXRD) pattern of NKPOC-DT exhibited two intense diffraction peaks at 2θ of $\sim 3.7^\circ$, $\sim 6.4^\circ$ and several weak yet discernible peaks at higher angles. The observed PXRD pattern of NKPOC-DT matched well with the reported CPOC-203^[22] and the simulated pattern obtained by geometrical and energetical optimization with materials studio (Figure S3). Furthermore, Fourier transform infrared (FT-IR) spectroscopy,^[22] solid-state ^{13}C nuclear magnetic resonance (^{13}C NMR) spectroscopy,^[23] ^1H nuclear magnetic resonance (^1H NMR) spectra^[20c,22] and time of flight mass

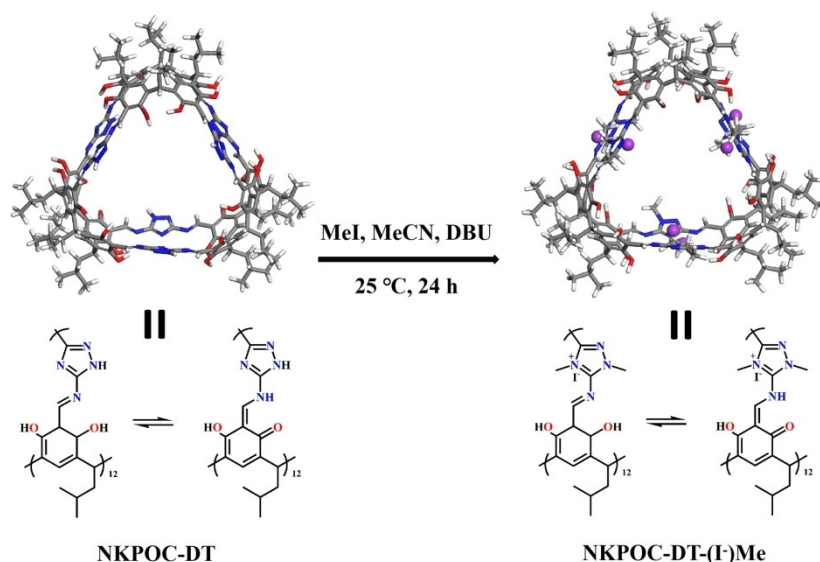


Figure 2. Schematic illustration of the synthesis of NKPOC-DT-(I⁻)Me. Note: DBU = 1,8-diazabicyclo[5.4.0]undec-7-ene, MeCN = Acetonitrile, MeI = Iodomethane.

spectrometry (TOF-MS) analysis^[22] further confirmed the successful incorporation of the designed structural moieties in NKPOC-DT (Figure S4–S7). NKPOC-DT-(I⁻)Me was obtained by reacting NKPOC-DT with iodomethane (MeI) using 1,8-diazabicyclo[5.4.0]undec-7-ene (DBU) as catalyst.^[24] PXRD analysis showed that diffraction peaks of NKPOC-DT-(I⁻)Me exhibited a slight changes but still retained the main peak compared with NKPOC-DT, indicating that the crystal structure of the functionalized POC remained intact (Figure 3a). The FT-IR spectra in Figure 3b shows two new bands at 1323 and 1705 cm⁻¹ corresponding to the C–N (N–CH₃), and C–N (N⁺–CH₃I⁻) that are not present in NKPOC-DT, implying the successful introduction of ionic sites onto the NKPOC-DT (Figure 3b).^[24c,25] Furthermore, the successful modification of ionic sites was further confirmed by ¹H NMR as illustrated by the appearance of two new signals at 4.39 ppm (h, N⁺–CH₃I⁻) and 3.70 ppm (g, N–CH₃) (Figure S8).^[25] Such conclusion can be also verified through solid-state ¹³C NMR studies, evidenced by the appearance of new signals at 53.7 (m, N⁺–CH₃I⁻) and 49.0 (l, N–CH₃) ppm in NKPOC-DT-(I⁻)Me (Figure 3c). In addition, X-ray photoelectron spectroscopy (XPS) analysis in NKPOC-DT-(I⁻)Me showed new N 1s (N⁺

–CH₃I⁻, 402.44 eV) and I 3d signals (629.39 eV for I 3d_{3/2} and 617.94 eV for I 3d_{5/2}) (Figure S9).^[26] These results thus confirm the ionic functional sites were successfully grafted onto NKPOC-DT. Energy-dispersive X-ray spectroscopy (EDS) mapping showed the uniform distribution of I element in NKPOC-DT-(I⁻)Me (Figure S10). Elementary analysis and TOF-MS results (Figure S11) imply that ~33% triazole was modified to form ionic sites in NKPOC-DT-(I⁻)Me.

Gas adsorption-desorption isotherms studies indicated that the installation of ionic sites onto NKPOC-DT led to a significant decrease of BET surface area from 1003 m²g⁻¹ for NKPOC-DT to 96 m²g⁻¹ for NKPOC-DT-(I⁻)Me (Figure S12). TGA demonstrated that NKPOC-DT-(I⁻)Me exhibited thermal stability up to 200 °C (Figure S13), which can meet the requirements for industrial nuclear waste treatment (i.e., 150 °C). Following treatment in acidic solution (pH=1) and boiling water (100 °C), NKPOC-DT-(I⁻)Me retained consistent PXRD and FT-IR patterns when compared to the as-prepared sample (Figure S14–S15), indicating good acid and hydrothermal stability. Such high thermal/chemical stabilities are the key to industrially capturing radioactive I₂.

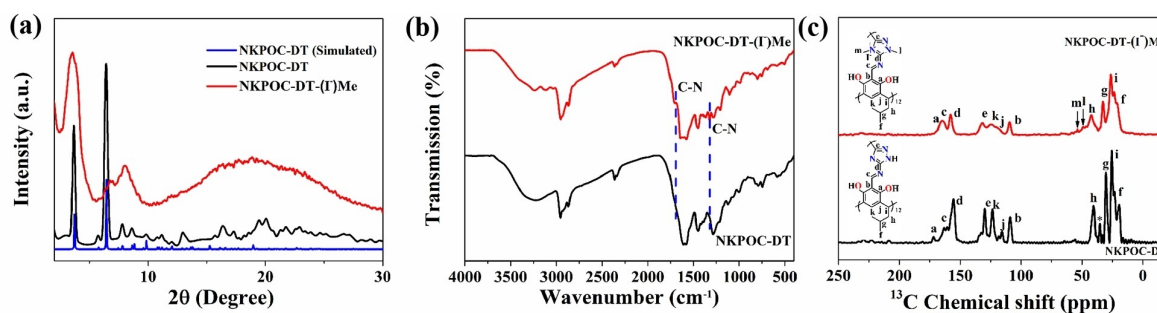


Figure 3. (a) PXRD patterns; (b) FT-IR spectra and (c) solid ¹³C NMR spectra of NKPOC-DT and NKPOC-DT-(I⁻)Me.

Iodine Capture Performance

Iodine capture experiments were conducted under simulated industrial conditions (150 °C, 150 ppmv of I₂). Typically, as-prepared samples (~5 mg) were placed into a thermo gravimetric analyzer, followed by passing 150 ppmv of I₂ steam with N₂ as a carrier gas. The adsorption amount was monitored by recording sample mass as a function of time. The NKPOC-DT-(I⁻)Me can absorb 48.35 wt % I₂ under industry-relevant condition (150 °C and 150 ppmv of I₂), a 3.2 times higher than the original NKPOC-DT with an uptake of 15.12 wt % under the same condition (Figure 4a and 4b). The I₂ capture performance of NKPOC-DT-(I⁻)Me also significantly surpasses all reported porous materials (Figure 4a-4c), including H₂L (highest I₂ adsorption capacity among metal-free zeolites, 0.16 wt %),^[16] PAF-1 (a porous organic polymer with an ultra-high surface area, 0.82 wt %),^[27] HPOC-101 (a porous organic cage with an ultra-high adsorption capacity of aqueous I₃⁻, 0.09 wt %),^[20c] ZIF-8 (a chemically stable MOF, 1.76 wt %),^[28] MFU-Cu(I) (a MOF with Cu(I) Sites, 20 wt %),^[29] Ag@MOR (a commonly used commercial adsorbent, 14 wt %),^[29] JUC-561 (a sulfur functionalized COF with redox sites, 20.03 wt %),^[12c] iCOF-AB-50 (an ionic COF, 8.27 wt %),^[12d] TGDM (a 2D guanidinium COF, 29.24 wt %),^[14] 4F-iCOF-TpBpy-I⁻ (a 2D COF with both ionic and Lewis base sites, 37 wt %).^[15] Additionally, the iodine loading NKPOC-DT-(I⁻)Me (I₂@NKPOC-DT-(I⁻)Me) can retain 78.9 % I₂ after nitrogen purging at 150 °C (Figure S16). And the retained I₂ is considered as being chemically bond to framework.^[14-15] According to the experimental results, each ionic site of NKPOC-DT-(I⁻)Me adsorbs ~1.62 I₂ molecules at 150 °C, which is 3.7 and 2.1 times higher than the 2D ionic COFs of TGDM (0.44 I₂ molecules per ionic site) and 4F-iCOF-TpBpy-I⁻

(0.76 I₂ molecules per ionic site) under the same conditions (Figure 4d). The lower I₂ uptakes for 2D ionic COFs in contrast to NKPOC-DT-(I⁻)Me may be attributed to the underutilized functional sites in confined space when adsorption, which thus results in the limitation of iodine adsorption ability for each binding sites. In contrast, NKPOC-DT-(I⁻)Me exhibits a highly dispersed ionic sites and sufficient space to efficiently bind and accommodate more I₂ molecules around functional adsorption sites thereby affording high adsorption performance.

Furthermore, adsorption kinetic is another crucial aspect for evaluating a sorbent's performance metrics in real-world applications. NKPOC-DT-(I⁻)Me demonstrated the remarkable adsorption rate of 0.013 min⁻¹, which is 1.2 and 1.6 times faster than that of benchmark materials (TGDM and 4F-iCOF-TpBpy-I⁻) under the same condition (Figure 4c, Figure S17). The remarkable adsorption kinetics of NKPOC-DT-(I⁻)Me can be attributed to the presence of strong ionic binding sites for capturing I₂ and the existence of accessible pores (7.6 Å), which is large enough to allow entrance of I₂ molecules with a molecular size of 3.96×3.96×6.62 Å (Figure S18). Together with the record-high uptake capacity, NKPOC-DT-(I⁻)Me thus sets a new benchmark for radioactive I₂ adsorbents under practical conditions (Figure 4c). These results thus highlight the advantages to develop new types of radioactive I₂ adsorbents with the features of highly dispersed/exposed functional sites and large accommodating space for guests.

NKPOC-DT-(I⁻)Me after I₂ adsorption can be recycled for five cycles by ionic exchange, which was demonstrated by the remained PXRD pattern, FT-IR spectra, XPS spectra, and uptake capacity (Figure S19-S22). Furthermore, the breakthrough curves demonstrate that the iodine vapor can be fully

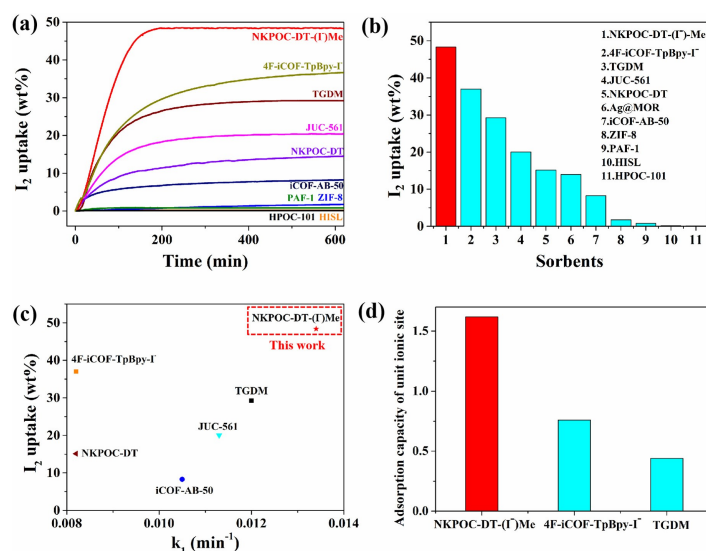


Figure 4. (a) Gravimetric measurements of I₂ adsorption on NKPOC-DT, NKPOC-DT-(I⁻)Me, TGDM, 4F-iCOF-TpBpy-I⁻, JUC-561, iCOF-AB-50, ZIF-8, HPOC-101, PAF-1, and H₂L as a function of time at 150 °C and 150 ppmv of I₂; (b) The comparison of the I₂ adsorption capacities of various high-performance adsorbents at 150 °C and 150 ppmv of I₂; (c) The comparison of I₂ saturation uptake amount and k₁ value for NKPOC-DT-(I⁻)Me at 150 °C and 150 ppmv of I₂ with other benchmark porous materials, including iCOF-AB-50, NKPOC-DT, JUC-561, TGDM, 4F-iCOF-TpBpy-I⁻; (d) The comparison of the number of iodine molecules adsorbed per ionic site for NKPOC-DT-(I⁻)Me at 150 °C and 150 ppmv of I₂ with benchmark materials of TGDM and 4F-iCOF-TpBpy-I⁻.

absorbed by NKPOC-DT-(I⁻)Me reaching an extraordinary adsorption capacity (49.2 wt % and 48.0 wt %) under both simulated dry and relative humidity (RH) of 50 % measurement conditions (50 mg of NKPOC-DT-(I⁻)Me, 150 °C, 150 ppmv I₂ in N₂ with a flow rate of 1.23 mg h⁻¹), which highlights its feasibility in the practical iodine capture under industry-relevant conditions (Scheme S1, Figure 5). Regulatory standards for nuclear processing facilities require a “decontamination factors” (DF) of >100–1000 (removal of 99.953 % of active species) for I₂ reprocessing, defined as the ratio of radioactivity before and after decontamination procedures.^[30] NKPOC-DT-(I⁻)Me achieves very high decontamination factors, ranging from 2170 to 9346 (Figure S23), corresponding to the removal of approximately 99.954–99.989 % I₂, which is significantly higher than the regulatory requirements for reprocessing facilities.^[30] These results indicate the high effectiveness of NKPOC-DT-(I⁻)Me in capturing radioactive I₂ from off-gas mixtures of nuclear waste. In addition, NKPOC-

DT can be prepared in large-scale (20.9 g of NKPOC-DT within 10 min) by a high pressure homogenization (HPH) method^[31] under room temperature (Figure S24–S27), which suggests its great potential for industrialization.

Adsorption Mechanism

The adsorption mechanism was validated by characterizing NKPOC-DT-(I⁻)Me before and after iodine saturation at 150 °C. The successful capture of I₂ can be observed by EDS mapping with a uniform distribution of I element (Figure S28). The PXRD pattern showed that the diffraction peaks of NKPOC-DT-(I⁻)Me completely disappeared after saturated with I₂, indicating the loss of structural order due to the installation of I₂ into the porous organic cages. No diffraction peaks of I₂ were observed, excluding the possibility that the high adsorption capacity was caused by the recrystallization of I₂ around the adsorbent (Figure S29).^[12a] Raman spectroscopy studies of NKPOC-DT-(I⁻)Me revealed new peaks of I₃⁻ (116, 137.9, and 147.5 cm⁻¹) and I₅⁻ (161.2, and 171.6 cm⁻¹) following I₂ loading, as compared to NKPOC-DT (Figure 6a), indicating the ionic modification of NKPOC-DT promotes the formation of polyiodides and thereby enhances the I₂ adsorption capacity.^[14,24a, 32] Furthermore, raman spectroscopy analysis revealed that iodine adsorption on NKPOC-DT-(I⁻)Me was calculated to be 1.62 iodine molecules per ionic site, based on the uptake results obtained after nitrogen purging at 150 °C (Figure S16, Figure S30), thus confirming predominant role of Coulombic interactions during the iodine adsorption process. The FT-IR spectra showed that the chemical shift of C–N (N⁺–CH₃I⁻) reached up to 15.5 cm⁻¹ after I₂ loading. This is significantly higher than the shifts of C–N (N–CH₃, 4.0 cm⁻¹), indicating that Coulomb interactions play a crucial role in

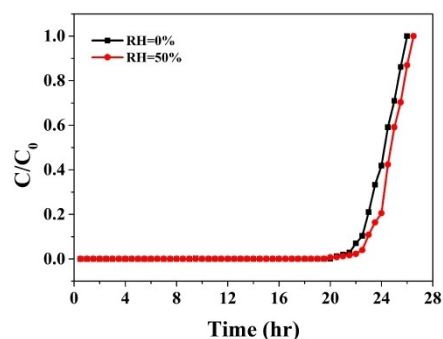


Figure 5. I₂ breakthrough profiles of NKPOC-DT-(I⁻)Me at 150 °C and 150 ppmv of dry (RH = 0%, black) and humid (RH = 50%, red) I₂.

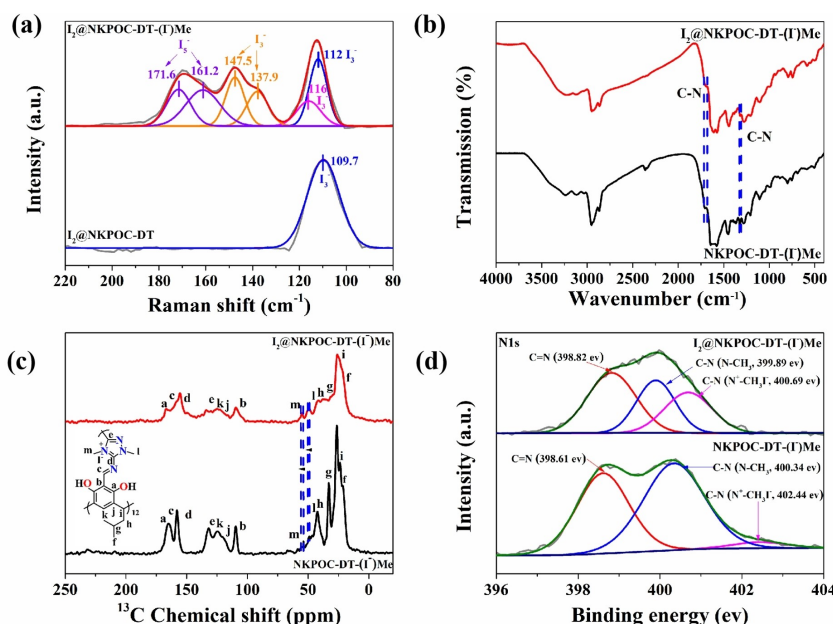


Figure 6. (a) Raman spectra of I₂@NKPOC-DT-(I⁻)Me and I₂@NKPOC-DT; (b) FT-IR spectra; (c) ¹³C CP-MAS NMR spectra; and (d) N1s spectra of NKPOC-DT-(I⁻)Me and I₂@NKPOC-DT-(I⁻)Me after nitrogen purging at 150 °C.

adsorption process (Figure 6b). Such result is also evidenced by a larger shift of m ($N^+-CH_3I^-$, 1.0 ppm) compare to 1 ($N-CH_3$, 0.2 ppm) carbon atom in the solid-state ^{13}C NMR spectra (Figure 6c).^[24a] Furthermore, the N 1s spectra (Figure 6d, Figure S31) showed that N in $N^+-CH_3I^-$ shifted from 402.44 eV to 400.69 eV after I_2 saturation. The chemical shift is much higher than that in C–N and C=N, indicating the importance of Coulomb interactions during adsorption process. The preferred adsorption configuration of I_2 at the ionic sites (I^-) than Lewis base sites (N) was explored by density functional theory (DFT) calculations, which was evidenced by the calculated binding energies for I_2 nearby ionic sites (I^-) (–1.14 eV) is 2.5 times higher than that of Lewis base sites I_2 nearby (N) (–0.46 eV) (Figure S32). In short, these findings strongly suggest that Coulomb interactions significantly contribute to the adsorption process under high temperature conditions.

Conclusion

In summary, we developed herein POC as an efficient platform for highly effective radioactive iodine capture under industrial conditions (typically $\geq 150^\circ C$, ≤ 150 ppmv of I_2). Due to highly dispersed/exposed binding sites and sufficient accommodating space for I_2 in POC, the constructed NKPOC-DT(I^-)Me exhibits a record-high I_2 uptake capacity of 48.35 wt %. It outperforms industrial silver-based adsorbents of Ag@MOR and the benchmark materials of TGDM and 4F-iCOF-TpBpy- I^- by 3.5, 1.6, and 1.3 times under the same conditions. In addition, each ionic site in NKPOC-DT(I^-)Me can adsorb ~ 1.62 I_2 under industrial conditions, which is the highest value among all porous adsorbents reported to date. Our work thus provides a new insight for effectively enhancing the adsorption ability of unit ion sites. Furthermore, NKPOC-DT(I^-)Me exhibits ultrafast adsorption kinetics ($k_1 = 0.013 \text{ min}^{-1}$), which is 1.2 and 1.6 times higher than the benchmark materials of TGDM and 4F-iCOF-TpBpy- I^- under identical conditions. NKPOC-DT(I^-)Me thus set a new benchmark for high-temperature radioactive I_2 adsorbents. This work may inspire the development of sorts of POCs for high-efficient radioiodine capture under industrial operating conditions.

Acknowledgements

This work was supported by the National Key R&D Program of China (2022YFA1503301), the National Natural Science Foundation of China (No. 21978138 and 22035003), the Fundamental Research Funds for the Central Universities (Nankai University), the Haihe Laboratory of Sustainable Chemical Transformations (YYJC202101), the China Postdoctoral Science Foundation (NO. 2022 M721702). Partial support from the Robert A. Welch Foundation (B-0027) (S.M.) is also acknowledged.

Conflict of Interest

The authors declare no conflict of interest.

Data Availability Statement

The data that support the findings of this study are available from the corresponding author upon reasonable request.

Keywords: porous organic cage · radioactive iodine capture · crystalline framework material · adsorption

- [1] a) E. Kintisch, *Science* **2005**, *310*, 1406; b) R. C. Ewing, F. N. von Hippel, *Science* **2009**, *325*, 151–152; c) H. Zhang, A. Li, K. Li, Z. Wang, X. Xu, Y. Wang, M. V. Sheridan, H.-S. Hu, C. Xu, E. V. Alekseev, Z. Zhang, P. Yan, K. Cao, Z. Chai, T. E. Albrecht-Schönzart, S. Wang, *Nature* **2023**, *616*, 482–487.
- [2] a) T. Pan, K. Yang, X. Dong, Y. Han, *J. Mater. Chem. A* **2023**, *11*, 5460–5475; b) X. Zhang, J. Maddock, T. M. Nenoff, M. A. Denecke, S. Yang, M. Schröder, *Chem. Soc. Rev.* **2022**, *51*, 3243–3262.
- [3] Y. Lan, M. Tong, Q. Yang, C. Zhong, *CrystEngComm* **2017**, *19*, 4920–4926.
- [4] Z. M. Wang, T. Arai, M. Kumagai, *Adsorpt. Sci. Technol.* **1999**, *17*, 255–268.
- [5] K. W. Chapman, P. J. Chupas, T. M. Nenoff, *J. Am. Chem. Soc.* **2010**, *132*, 8897–8899.
- [6] a) B. J. Riley, J. D. Vienna, D. M. Strachan, J. S. McCloy, J. L. Jerden Jr., *J. Nucl. Mater.* **2016**, *470*, 307–326; b) T. Pan, K. Yang, X. Dong, S. Zuo, C. Chen, G. Li, A.-H. Emwas, H. Zhang, Y. Han, *Nat. Commun.* **2024**, *15*, 2630.
- [7] K. Jie, Y. Zhou, E. Li, Z. Li, R. Zhao, F. Huang, *J. Am. Chem. Soc.* **2017**, *139*, 15320–15323.
- [8] a) B. Pemberton, W. Ng, *Public Money & Manage.* **2019**, *40*, 335–341; b) W. J. Davis, J. M. Van Dyke, *Marine Policy* **1990**, *14*, 467–476.
- [9] a) D. Li, D. I. Kaplan, K. A. Price, J. C. Seaman, K. Roberts, C. Xu, P. Lin, W. Xing, K. Schwehr, P. H. Santschi, *J. Environ. Radioact.* **2019**, *208–209*, 106017; b) C. Du, B. Liu, J. Hu, H. Li, *Mater. Lett.* **2021**, *285*, 129137.
- [10] a) H.-L. Xia, K. Zhou, L. Yu, H. Wang, X.-Y. Liu, J. Li, *Inorg. Chem.* **2022**, *61*, 17109–17114; b) W. Zhang, J. Zhang, X. Dong, M. Li, Q. He, S. Zhao, L. Xie, *Chem. Eng. J.* **2023**, *461*, 142058; c) X. Wang, M. Li, J. Zhang, X. He, J. C. Crittenden, W. Zhang, *ACS Appl. Nano Mater.* **2023**, *6*, 7206–7217; d) X. Zhang, I. da Silva, H. G. W. Godfrey, S. K. Callear, S. A. Sapchenko, Y. Cheng, I. Vitorica-Yrezabal, M. D. Frogley, G. Cinque, C. C. Tang, C. Giacobbe, C. Dejoie, S. Rudić, A. J. Ramirez-Cuesta, M. A. Denecke, S. Yang, M. Schröder, *J. Am. Chem. Soc.* **2017**, *139*, 16289–16296; e) Y. Sun, D.-F. Lu, K. Wu, T. Zhou, F. Wang, J. Zhang, *Cryst. Growth Des.* **2021**, *21*, 28–32; f) S.-T. Wang, Y.-J. Liu, C.-Y. Zhang, F. Yang, W.-H. Fang, J. Zhang, *Chem. - Eur. J.* **2023**, *29*, e202202638; g) S. Tian, Z. Yi, J. Chen, S. Fu, *J. Hazard. Mater.* **2023**, *443*, 130236; h) S. Yao, W.-H. Fang, Y. Sun, S.-T. Wang, J. Zhang, *J. Am. Chem. Soc.* **2021**, *143*, 2325–2330; i) C.-H. Liu, W.-H. Fang, Y. Sun, S. Yao, S.-T. Wang, D. Lu, J. Zhang, *Angew. Chem. Int. Ed.* **2021**, *60*, 21426–21433; j) Y.-J. Liu, Y.-F. Sun, S.-H. Shen, S.-T. Wang, Z.-H. Liu, W.-H. Fang, D. S. Wright, J. Zhang, *Nat. Commun.* **2022**, *13*, 6632; k) Z.-J. Li, Y. Ju, B. Yu, X. Wu, H. Lu, Y. Li, J. Zhou, X. Guo, Z.-H. Zhang, J. Lin, J.-Q. Wang, S. Wang, *Chem. Commun.* **2020**, *56*, 6715–6718; l) Y. Zhang, L. He, T. Pan, J. Xie, F. Wu, X. Dong, X. Wang, L.

- Chen, S. Gong, W. Liu, L. Kang, J. Chen, L. Chen, L. Chen, Y. Han, S. Wang, *CCS Chem.* **2023**, *5*, 1540–1548.
- [11] a) W. Xie, D. Cui, S.-R. Zhang, Y.-H. Xu, D.-L. Jiang, *Mater. Horiz.* **2019**, *6*, 1571–1595; b) J. Zhang, N. Pu, M. Li, W. Sang, Q. He, Q. Tian, W. Zhang, *Sep. Purif. Technol.* **2024**, *328*, 125052; c) K. Su, W. Wang, B. Li, D. Yuan, *ACS Sustainable Chem. Eng.* **2018**, *6*, 17402–17409; d) Z. Yan, Y. Yuan, Y. Tian, D. Zhang, G. Zhu, *Angew. Chem. Int. Ed.* **2015**, *54*, 12733–12737; e) Z. Ma, L. He, F. Zhao, Y. Tao, W. Sun, B. Tai, Q. Guo, W. Zhang, F. Peng, J. Chen, B. Li, L. Chen, X. Dai, Z. Chai, S. Wang, *Sep. Purif. Technol.* **2024**, *345*, 127321.
- [12] a) Y. Xie, T. Pan, Q. Lei, C. Chen, X. Dong, Y. Yuan, W. A. Maksoud, L. Zhao, L. Cavallo, I. Pinnau, Y. Han, *Nat. Commun.* **2022**, *13*, 2878; b) C. Wang, Y. Wang, R. Ge, X. Song, X. Xing, Q. Jiang, H. Lu, C. Hao, X. Guo, Y. Gao, D. Jiang, *Chem. Eur. J.* **2018**, *24*, 585–589; c) L. He, L. Chen, X. Dong, S. Zhang, M. Zhang, X. Dai, X. Liu, P. Lin, K. Li, C. Chen, T. Pan, F. Ma, J. Chen, M. Yuan, Y. Zhang, L. Chen, R. Zhou, Y. Han, Z. Chai, S. Wang, *Chem* **2021**, *7*, 699–714; d) Y. Xie, T. Pan, Q. Lei, C. Chen, X. Dong, Y. Yuan, J. Shen, Y. Cai, C. Zhou, I. Pinnau, Y. Han, *Angew. Chem. Int. Ed.* **2021**, *60*, 22432–22440; e) J. Chang, H. Li, J. Zhao, X. Guan, C. Li, G. Yu, V. Valtchev, Y. Yan, S. Qiu, Q. Fang, *Chem. Sci.* **2021**, *12*, 8452–8457; f) T. Liu, Y. Zhao, M. Song, X. Pang, X. Shi, J. Jia, L. Chi, G. Lu, *J. Am. Chem. Soc.* **2023**, *145*, 2544–2552; g) K. Cheng, H. Li, J.-R. Wang, P.-Z. Li, Y. Zhao, *Small* **2023**, *19*, 2301998; h) P. Wang, Q. Xu, Z. Li, W. Jiang, Q. Jiang, D. Jiang, *Adv. Mater.* **2018**, *30*, 1801991; i) Y. Xie, Q. Rong, F. Mao, S. Wang, Y. Wu, X. Liu, M. Hao, Z. Chen, H. Yang, G. I. N. Waterhouse, S. Ma, X. Wang, *Nat. Commun.* **2024**, *15*, 2671; j) M. Hao, Y. Xie, M. Lei, X. Liu, Z. Chen, H. Yang, G. I. N. Waterhouse, S. Ma, X. Wang, *J. Am. Chem. Soc.* **2024**, *146*, 1904–1913; k) M. Yuan, F. Ma, L. Chen, B. Li, X. Dai, J. Shu, L. He, J. Chen, S. Lin, G. Xie, Z. Chai, S. Wang, *J. Am. Chem. Soc.* **2024**, *146*, 1250–1256.
- [13] a) X. Jiang, X. Cui, A. J. E. Duncan, L. Li, R. P. Hughes, R. J. Staples, E. V. Alexandrov, D. M. Proserpio, Y. Wu, C. Ke, *J. Am. Chem. Soc.* **2019**, *141*, 10915–10923; b) Y. Lin, X. Jiang, S. T. Kim, S. B. Alahakoon, X. Hou, Z. Zhang, C. M. Thompson, R. A. Smaldone, C. Ke, *J. Am. Chem. Soc.* **2017**, *139*, 7172–7175; c) Y. Wang, Y. Jin, W. Xian, X. Zuo, S. Wang, Q. Sun, *J. Mater. Chem. A* **2022**, *10*, 18730–18736.
- [14] Z. Zhang, X. Dong, J. Yin, Z.-G. Li, X. Li, D. Zhang, T. Pan, Q. Lei, X. Liu, Y. Xie, F. Shui, J. Li, M. Yi, J. Yuan, Z. You, L. Zhang, J. Chang, H. Zhang, W. Li, Q. Fang, B. Li, X.-H. Bu, Y. Han, *J. Am. Chem. Soc.* **2022**, *144*, 6821–6829.
- [15] F. Shui, Q. Lei, X. Dong, T. Pan, Z. Zhang, J. Li, M. Yi, L. Zhang, X. Liu, Z. You, S. Yang, R. Yang, H. Zhang, J. Li, Z. Shi, J. Yin, B. Li, X.-H. Bu, *Chem. Eng. J.* **2023**, *468*, 143525.
- [16] B. Li, X. Dong, H. Wang, D. Ma, K. Tan, S. Jensen, B. J. Deibert, J. Butler, J. Cure, Z. Shi, T. Thonhauser, Y. J. Chabal, Y. Han, J. Li, *Nat. Commun.* **2017**, *8*, 1–9.
- [17] a) Z. Wang, S. Zhang, Y. Chen, Z. Zhang, S. Ma, *Chem. Soc. Rev.* **2020**, *49*, 708–735; b) X. Guan, F. Chen, Q. Fang, S. Qiu, *Chem. Soc. Rev.* **2020**, *49*, 1357–1384; c) X. Guan, F. Chen, S. Qiu, Q. Fang, *Angew. Chem. Int. Ed.* **2023**, *62*, e202213203.
- [18] a) K. Su, W. Wang, S. Du, C. Ji, D. Yuan, *Nat. Commun.* **2021**, *12*, 3703; b) L. Feng, Y. Xie, W. Wang, K. Su, D. Yuan, *J. Mater. Chem. A* **2023**, *11*, 25316–25321; c) E. Martínez-Ahumada, D. He, V. Berryman, A. López-Olvera, M. Hernandez, V. Jancik, V. Martis, M. A. Vera, E. Lima, D. J. Parker, A. I. Cooper, I. A. Ibarra, M. Liu, *Angew. Chem. Int. Ed.* **2021**, *60*, 17556–17563; d) A. He, Z. Jiang, Y. Wu, H. Hussain, J. Rawle, M. E. Briggs, M. A. Little, A. G. Livingston, A. I. Cooper, *Nat. Mater.* **2022**, *21*, 463–470; e) T. Hasell, M. Miklitz, A. Stephenson, M. A. Little, S. Y. Chong, R. Clowes, L. Chen, D. Holden, G. A. Tribello, K. E. Jelfs, A. I. Cooper, *J. Am. Chem. Soc.* **2016**, *138*, 1653–1659.
- [19] a) X. Yang, J.-K. Sun, M. Kitta, H. Pang, Q. Xu, *Nat. Catal.* **2018**, *1*, 214–220; b) J.-K. Sun, W.-W. Zhan, T. Akita, Q. Xu, *J. Am. Chem. Soc.* **2015**, *137*, 7063–7066; c) N. Xu, K. Su, E.-S. M. El-Sayed, Z. Ju, D. Yuan, *Chem. Sci.* **2022**, *13*, 3582–3588.
- [20] a) X. Yang, Z. Ullah, J. F. Stoddart, C. T. Yavuz, *Chem. Rev.* **2023**, *123*, 4602–4634; b) T. Hasell, A. I. Cooper, *Nat. Rev. Mater.* **2016**, *1*, 16053; c) M. Yang, F. Qiu, E.-S. M. El-Sayed, W. Wang, S. Du, K. Su, D. Yuan, *Chem. Sci.* **2021**, *12*, 13307–13315; d) T. Hasell, M. Schmidtman, A. I. Cooper, *J. Am. Chem. Soc.* **2011**, *133*, 14920–14923; e) C. Liu, W. Li, Y. Liu, H. Wang, B. Yu, Z. Bao, J. Jiang, *Chem. Eng. J.* **2022**, *428*, 131129; f) C. Liu, Y. Jin, Z. Yu, L. Gong, H. Wang, B. Yu, W. Zhang, J. Jiang, *J. Am. Chem. Soc.* **2022**, *144*, 12390–12399; g) J. Yang, S.-J. Hu, L.-X. Cai, L.-P. Zhou, Q.-F. Sun, *Nat. Commun.* **2023**, *14*, 6082.
- [21] a) M. E. Briggs, A. I. Cooper, *Chem. Mater.* **2017**, *29*, 149–157; b) H. Wang, Y. Jin, N. Sun, W. Zhang, J. Jiang, *Chem. Soc. Rev.* **2021**, *50*, 8874–8886; c) K. Su, W. Wang, S. Du, C. Ji, M. Zhou, D. Yuan, *J. Am. Chem. Soc.* **2020**, *142*, 18060–18072.
- [22] L. Feng, Y. Xie, W. Wang, K. Su, D. Yuan, *J. Mater. Chem. A* **2023**, *11*, 25316–25321.
- [23] a) S. Haldar, K. Roy, S. Nandi, D. Chakraborty, D. Puthusseri, Y. Gawli, S. Ogale, R. Vaidhyanathan, *Adv. Energy Mater.* **2018**, *8*, 1702170; b) H. Li, H. Huang, X. Yan, C. Liu, L. Li, *Mater. Chem. Phys.* **2021**, *263*, 124295.
- [24] a) X. Pan, E. Lacôte, J. Lalevée, D. P. Curran, *J. Am. Chem. Soc.* **2012**, *134*, 5669–5674; b) X. Wang, B. Zhu, Y. Liu, Q. Wang, *ACS Catal.* **2022**, *12*, 2522–2531; c) J. L. Belletire, R. A. Bills, S. A. Shackelford, *Synth. Commun.* **2008**, *38*, 738–745.
- [25] S.-H. Ueng, L. Fensterbank, E. Lacôte, M. Malacria, D. P. Curran, *Org. Lett.* **2010**, *12*, 3002–3005.
- [26] a) T. Stamenković, N. Bundaleski, T. Barudžija, I. Validžić, V. Lojpur, *Appl. Surf. Sci.* **2021**, *567*, 150822; b) G. Zhao, Y. Li, G. Zhu, J. Shi, T. Lu, L. Pan, *ACS Sustainable Chem. Eng.* **2019**, *7*, 12052–12060; c) X. Liu, C. Zhu, J. Yin, J. Li, Z. Zhang, J. Li, F. Shui, Z. You, Z. Shi, B. Li, X.-H. Bu, A. Nafady, S. Ma, *Nat. Commun.* **2022**, *13*, 2132.
- [27] C. Pei, T. Ben, S. Xu, S. Qiu, *J. Mater. Chem. A* **2014**, *2*, 7179–7187.
- [28] a) J. T. Hughes, D. F. Sava, T. M. Nenoff, A. Navrotsky, *J. Am. Chem. Soc.* **2013**, *135*, 16256–16259; b) K. W. Chapman, G. J. Halder, P. J. Chupas, *J. Am. Chem. Soc.* **2009**, *131*, 17546–17547.
- [29] T. Pan, K. Yang, X. Dong, J. Tao, Y. Han, *ACS Materials Lett.* **2024**, *6*, 2794–2801.
- [30] N. Soelberg, T. Watson, Report No. FCRD-SWF-2011-000316, INL/EXT-11-23191, **2011**.
- [31] X. Liu, A. Wang, C. Wang, J. Li, Z. Zhang, A. M. Al-Enizi, A. Nafady, F. Shui, Z. You, B. Li, Y. Wen, S. Ma, *Nat. Commun.* **2023**, *14*, 7022.
- [32] L. Zhang, J. Li, H. Zhang, Y. Liu, Y. Cui, F. Jin, K. Wang, G. Liu, Y. Zhao, Y. Zeng, *Chem. Commun.* **2021**, *57*, 5558–5561.

Manuscript received: June 17, 2024

Revised manuscript received: July 22, 2024

Accepted manuscript online: July 30, 2024

Version of record online: September 23, 2024